



## NRC Publications Archive Archives des publications du CNRC

### High-precision gravimetric technique for determining the solubility and diffusivity of gases in polymers

Wong, Betty; Zhang, Zhiyi; Handa, Y. Paul

This publication could be one of several versions: author's original, accepted manuscript or the publisher's version. / La version de cette publication peut être l'une des suivantes : la version prépublication de l'auteur, la version acceptée du manuscrit ou la version de l'éditeur.

For the publisher's version, please access the DOI link below. / Pour consulter la version de l'éditeur, utilisez le lien DOI ci-dessous.

#### **Publisher's version / Version de l'éditeur:**

[http://dx.doi.org/10.1002/\(SICI\)1099-0488](http://dx.doi.org/10.1002/(SICI)1099-0488)

*Journal of Polymer Science Part B: Polymer Physics*, 36, 12, pp. 2025-2032, 1998-12-07

#### **NRC Publications Record / Notice d'Archives des publications de CNRC:**

<http://nparc.cisti-icist.nrc-cnrc.gc.ca/npsi/ctrl?action=rtdoc&an=14299098&lang=en>

<http://nparc.cisti-icist.nrc-cnrc.gc.ca/npsi/ctrl?action=rtdoc&an=14299098&lang=fr>

Access and use of this website and the material on it are subject to the Terms and Conditions set forth at

[http://nparc.cisti-icist.nrc-cnrc.gc.ca/npsi/jsp/nparc\\_cp.jsp?lang=en](http://nparc.cisti-icist.nrc-cnrc.gc.ca/npsi/jsp/nparc_cp.jsp?lang=en)

READ THESE TERMS AND CONDITIONS CAREFULLY BEFORE USING THIS WEBSITE.

L'accès à ce site Web et l'utilisation de son contenu sont assujettis aux conditions présentées dans le site

[http://nparc.cisti-icist.nrc-cnrc.gc.ca/npsi/jsp/nparc\\_cp.jsp?lang=fr](http://nparc.cisti-icist.nrc-cnrc.gc.ca/npsi/jsp/nparc_cp.jsp?lang=fr)

LISEZ CES CONDITIONS ATTENTIVEMENT AVANT D'UTILISER CE SITE WEB.

Contact us / Contactez nous: [nparc.cisti@nrc-cnrc.gc.ca](mailto:nparc.cisti@nrc-cnrc.gc.ca).



# High-Precision Gravimetric Technique for Determining the Solubility and Diffusivity of Gases in Polymers

BETTY WONG, ZHIYI ZHANG, Y. PAUL HANDA

Institute for Chemical Process and Environmental Technology, National Research Council of Canada, Ottawa, Ontario, Canada K1A 0R6

Received 29 October 1997; revised 20 February 1998; accepted 23 February 1998

**ABSTRACT:** An *in situ* gravimetric technique, employing an electrobalance, is described for determining the solubility and diffusivity of gases in polymers over extended ranges of temperature and pressure. Solubilities of CO<sub>2</sub> in polystyrene at 35°C were measured as a test case; the results are in excellent agreement with the literature values determined by the pressure decay method. Solubility and diffusivity results are also reported for PVC-CO<sub>2</sub> at 35°C and for PS-1,1,1,2-tetrafluoroethane at 30, 90, and 120°C. A comparison with other studies shows the *in situ* method to be more efficient and precise than the ones based on weighing the gas-saturated polymer under ambient conditions. The kinetics of gas sorption were analyzed in terms of two data reduction techniques to derive diffusion coefficients. © 1998 John Wiley & Sons, Inc. *J Polym Sci B: Polym Phys* 36: 2025–2032, 1998

**Keywords:** polymer; gas; solubility; diffusivity

## INTRODUCTION

Solubility and diffusivity of a gas in a polymer are important parameters in foam processing, and in establishing the intrinsic gas transport characteristics of gas separation membranes and barrier materials. Diffusion coefficients are rarely measured directly; instead, they are derived either from the kinetics of gas sorption<sup>1,2</sup> or from the time lags associated with steady-state permeability across a homogeneous film of known thickness.<sup>1</sup> The techniques employing permeability measurements are often used by membranologists to obtain diffusion coefficients<sup>3</sup> whereas investigators working on developing foaming processes use sorption kinetics to that purpose.<sup>4</sup> In the latter case, an often used technique<sup>5</sup> to obtain solubilities and diffusivities is to place the polymer sample in a pressure vessel, degas the sys-

tem, and then pressurize it with the desired gas. The sample is removed from the vessel periodically and weighed until a constant weight is obtained. From these results, the kinetics of sorption (and the diffusion coefficient) and equilibrium solubilities are obtained. A major source of error in these measurements is the escape of gas during the various handling procedures involved in weighing the sample. Furthermore, it is not possible to assess the magnitude of this error as it depends on the nature of the polymer, its size and shape (surface to volume ratio), and the nature of the gas. In general, this method is very time consuming for slow diffusants and the results often have large uncertainties for fast diffusants.

High precision solubilities usually are obtained using either the pressure decay method<sup>6</sup> or the gravimetric method using an electrobalance.<sup>7</sup> In the former technique, the polymer is placed in a reservoir of known volume and the change in pressure due to dissolution of the gas is measured relative to a matched empty reference-volume. This technique requires rather careful calibrations, and can be used only for gases whose equation of states

Correspondence to: Y. P. Handa (E-mail: paul.handa@nrc.ca)

*Journal of Polymer Science: Part B: Polymer Physics*, Vol. 36, 2025–2032 (1998)  
© 1998 John Wiley & Sons, Inc. CCC 0887-6266/98/122025-08

are accurately known. The gravimetric technique employing an electronic microbalance has been used successfully for obtaining gas solubilities over limited ranges of temperature and pressure. We describe an *in situ* high-pressure gravimetric technique that extends the temperature and pressure ranges previously employed using an electrobalance,<sup>7</sup> and that overcomes the limitations encountered previously with the pressure decay and the ambient-pressure gravimetric techniques.

## EXPERIMENTAL

### Polymer Samples

The polymers investigated were polystyrene, PS (Scott C-35,  $M_w = 258,000$ ,  $M_n = 103,000$ ,  $T_g = 104^\circ\text{C}$ ), filled poly(vinylchloride), FPVC, containing 7.5 wt % additive (Royal Plastics Geon 103EPF76) with a  $T_g = 61^\circ\text{C}$ , and unplasticized poly(vinylchloride), UPVC, from Goodfellow with a  $T_g = 77^\circ\text{C}$ . The PS films, about 100  $\mu\text{m}$  thick, were cast from a 3 wt % solution in chloroform, using the procedure described elsewhere.<sup>8</sup> After 3–5 days, the films were removed from the casting rings and dried under vacuum. The  $T_g$  of the film was monitored throughout the drying process using a differential scanning calorimeter (TA Instruments, DSC 2910). This was continued until the  $T_g$  of the film reached that of the original PS powder. The films were then annealed  $10^\circ\text{C}$  above  $T_g$  to remove any residual stresses and to assure that the films had the same thermal history. The FPVC films were melt pressed at  $190^\circ\text{C}$  and 190 atm to a thickness of 300  $\mu\text{m}$  and air quenched, whereas the UPVC film was used as received.

High purity  $\text{CO}_2$  (SFE grade) was obtained from Air Products, and 1,1,1,2-tetrafluoroethane (HFC134a) was obtained from Elf Atochem North America.

### Solubility Measurements

A Cahn D110 electronic microbalance was used to measure gas solubilities, and to determine diffusion coefficients. The balance was mounted on a vibration-free stand as illustrated in Figure 1. The weighing unit was contained within a heavy walled stainless steel dome rated to 120 atm. The dome can be lifted by the pulley system to allow access to the weighing unit. A floating plate supported by three screws kept the weighing unit leveled at all times. A matched pair of stainless

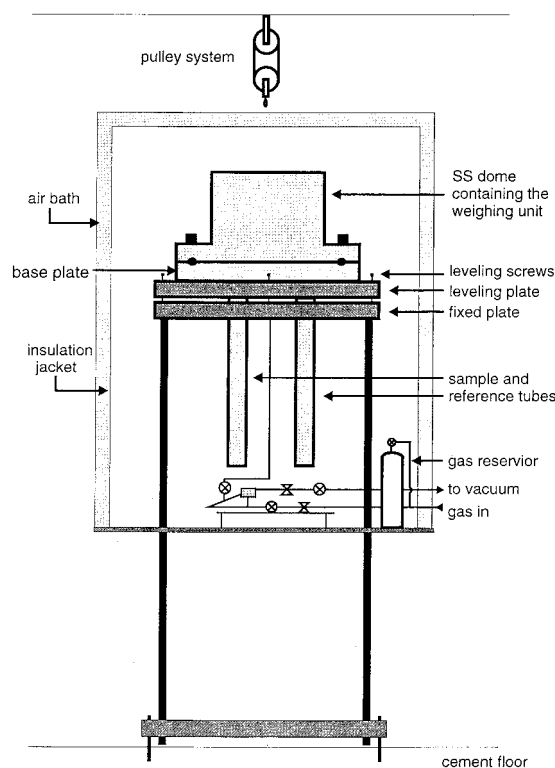


**Figure 1.** A schematic of the electrobalance setup.

steel tubes housed the reference and the sample vessels made of quartz and suspended from the two arms of the weighing unit by nichrome wires. The balance was connected to vacuum and gas lines through a series of pneumatic and metering valves as shown in Figure 2. The entire system, including the valves and a gas reservoir, was enclosed in an air thermostat controllable to  $(120 \pm 0.1)^\circ\text{C}$ . Measurements at temperatures from 120 to  $300^\circ\text{C}$  can be made by circulating thermostatted oil through the jackets surrounding the sample and the reference tubes. Samples of different size and shape (up to 35  $\text{cm}^3$  or 100 g) can be used. For sample sizes  $< 10$  g, the resolution of the balance is 10  $\mu\text{g}$ .

Approximately 1 g of sample, in the form of 12 mm diameter disks, was placed in the sample vessel. Filter paper disks, also 12 mm in diameter, were placed between the polymer disks to avoid the latter fusing together at temperatures close to or above  $T_g$ . A matched vessel containing the same number of filter paper disks as on the sample side and glass beads weighing approximately the same as the polymer sample were installed on the reference side. An appropriate amount of nichrome wire was then added to the sample vessel such that the mass and volume of the two

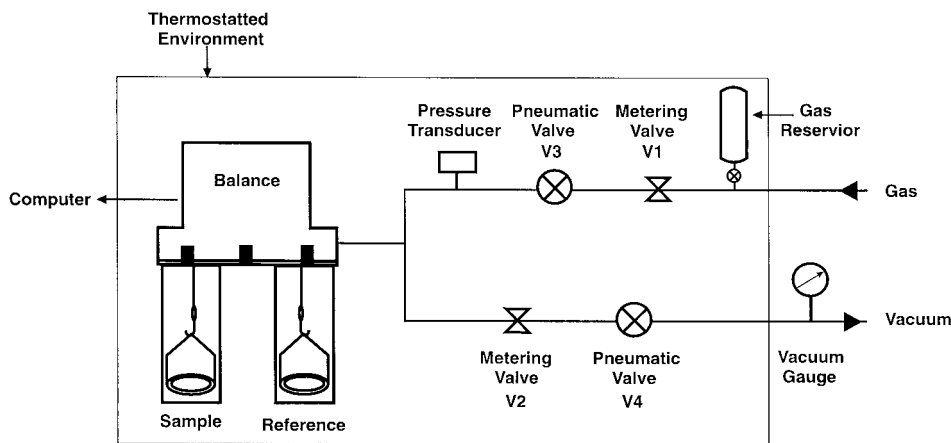


**Figure 2.** A schematic of the gas handling and temperature control systems.

vessels were as matched as possible in order to minimize the effect of buoyancy.

Metering valves V1 and V2 were preset to allow slow pressurization or depressurization of the system. A rapid pressurization/depressurization tended not only to shift the zero setting of the balance but also led to erratic changes in mass gain/loss due to fluctuations in the gas temperature. Once optimum settings were found for V1 and V2, pressurization/depressurization was performed by controlling remotely the pneumatic valves V3 and V4.

The sample was degassed for three days or until there was no further change in mass. Before commencing the sorption experiment, the gas was preheated to the desired temperature in a reservoir to minimize shock to the system. Mass readings were collected for 5 min to obtain a good baseline and accurate initial time for kinetic studies. The gas was then introduced to the desired pressure as indicated by the pressure transducer. The mass gain was recorded every 10 s until a constant value was obtained. An additional amount of gas was then introduced to raise the pressure to the next value, and the kinetics of sorption and new equilibrium mass were established again. This was continued until measurements over the desired pressure range were completed at a given temperature. For HFC134a at subcritical temperatures, the maximum pressure used was 90% of the saturation vapor pressure to ensure that the HFC134a did not condense within the system. The desorption runs were conducted in a similar fashion by releasing the gas in steps until the pressure in the system was back to almost zero. Because of the large volume associated with the system, about 2 liters, the pressure remained vir-

tually constant during the gas sorption and desorption runs.

Blank runs were conducted under the same conditions used for the solubility measurements. In these runs, empty cells matched precisely in mass and volume were employed to determine shift in the balance zero as a function of pressure. The equilibrium mass readings obtained in the solubility experiments were then corrected for the zero shift. Corrections for buoyancy due to the small volume difference between the sample and reference sides that developed as the polymer dilated due to dissolution of the gas were also made and are described below.

### Data Analysis

The diffusion coefficients were calculated using two methods. The first is a hybrid method based on the gas transport kinetics at short and long times. For thin, flat film geometry, the kinetics of Fickian sorption (desorption) are given by eqs. (1) and (2), respectively

$$\frac{M_t}{M_\infty} = \frac{4}{h} \left( \frac{Dt}{\pi} \right)^{1/2} + \frac{8}{h} (Dt)^{1/2} \sum_{n=1}^{\infty} (-1)^n \operatorname{ierfc} \left( \frac{nh}{2(Dt)^{1/2}} \right) \quad (1)$$

$$\frac{M_t}{M_\infty} = 1 - \frac{8}{\pi^2} \sum_{n=0}^{\infty} \frac{1}{(2n+1)^2} \times \exp \left( \frac{-(2n+1)^2 \pi^2 Dt}{h^2} \right) \quad (2)$$

where  $M_t$  and  $M_\infty$  are the masses sorbed at time  $t$  and  $t = \infty$ , respectively,  $h$  is the film thickness, and  $D$  is the diffusion coefficient. Equation (1) converges rapidly at short times, whereas eq. (2) converges rapidly at long times. Equation (1) truncated after the first term on the right-hand side, and eq. (2) truncated after the first two terms on the right-hand side are often used to obtain  $D$ . However, these techniques are not satisfactory as they do not utilize the entire kinetic curve.<sup>1,2</sup> As suggested recently,<sup>2</sup> the preferred method is to use the form

$$\frac{M_t}{M_\infty} = \phi(x)f(x) + [1 - \phi(x)]g(x) \quad (3)$$

where  $f(x)$  and  $g(x)$  represent the first term in eq. (1) and the first two terms in eq. (2), respectively,  $x = Dt/h^2$ , and  $\phi(x)$  is a weighting function defined as:

$$\begin{aligned} \phi(x) &= 1, & x &\leq 0.05326 \\ \phi(x) &= 0, & x &> 0.05326. \end{aligned}$$

The obvious advantage of using eq. (3), the hybrid form, is that it requires only the kinetic data; it can be used even if the entire kinetic curve is not known, and uncoupled values of  $D$  and  $M_\infty$  can be obtained easily.

The second technique used to determine diffusion coefficients is known as the moment method<sup>1</sup>

$$\tau = \int_0^\infty \left(1 - \frac{M_t}{M_\infty}\right) dt \quad (4)$$

$$D = \frac{h^2}{12\tau} \quad (5)$$

where  $h$  is the film thickness,  $\tau$  is the moment,  $M_t$  is the mass at time  $t$ , and  $M_\infty$  is the equilibrium mass. This technique also utilizes the entire kinetic curve; however, knowledge of the equilibrium mass is necessary.

As noted above, the equilibrium solubilities were corrected for the zero shift. The resulting values were then corrected for buoyancy imbalance between the sample and reference sides. The buoyancy correction depends on the volume difference between the sample and reference sides at the start of the experiment,  $\Delta V_i$ , and on the additional volume difference,  $\Delta V_d$ , that develops as the polymer is increasingly dilated by the dis-

solved gas. Note that  $\Delta V_d$  is a function of the gas pressure. The overall buoyancy correction is given by

$$w_b = \rho_g(\Delta V_i + \Delta V_d) \quad (6)$$

where  $\rho_g$  is the density of the gas. For CO<sub>2</sub>,  $\rho_g$  was obtained from the IUPAC recommended equation of state.<sup>9</sup> For HFC134a,  $\rho_g$  was calculated using the equation of state

$$pV = RT + Bp \quad (7)$$

where  $V$  is the molar volume and  $B$  is the second virial coefficient. The latter for HFC134a, at various temperatures, was obtained from a corresponding states plot<sup>10</sup> of  $B/V_c$  against  $T/T_c$  for various fluorocarbons;  $V_c$  and  $T_c$  being the critical volume and temperature, respectively. The second virial coefficients for the various fluorocarbons were taken from the literature.<sup>11</sup> For HFC134a, values of  $B$  thus obtained were  $-439$ ,  $-277$ , and  $-236$  cm<sup>3</sup> mol<sup>-1</sup> at 30, 90, and 120°C, respectively.

The corrected solubility is then given by

$$C = \frac{w_a + w_b}{M_P} \quad (8)$$

where  $M_P$  is the mass of the polymer,  $w_a$  is the apparent mass gain as recorded by the electrobalance and corrected for the zero shift, and  $C$  is the solubility in mass of gas dissolved in unit mass of polymer.

It has been well established that, for a glassy polymer, the gas sorbed in Henry's region only contributes to dilation.<sup>12</sup> The change in volume due to dilation was calculated by multiplying the moles of gas sorbed in the Henrian sites by the partial molar volume of the gas in the polymer,  $\bar{V}_g$ . Kamiya et al.<sup>13</sup> have shown that a linear relationship exists between  $\bar{V}_g$  and van der Waals volume of various gases. However, there usually is some ambiguity involved in calculating the van der Waals volumes. We found that  $\bar{V}_g$  correlates well with the molar volume of the gas at its critical point,  $V_c$ . This correlation is shown in Figure 3, and is preferred over that based on the van der Waals volumes as precise values of  $V_c$  are easily available.<sup>14</sup>  $\bar{V}_g$  values used in Figure 3 are for Ne, Ar, Kr, Xe, H<sub>2</sub>, N<sub>2</sub>, O<sub>2</sub>, CO<sub>2</sub>, N<sub>2</sub>O, CH<sub>4</sub>, C<sub>2</sub>H<sub>4</sub>, C<sub>2</sub>H<sub>6</sub>, C<sub>3</sub>H<sub>6</sub>, and C<sub>3</sub>H<sub>8</sub> in the rubbery state of polycarbonate, polyethylene, polybutadiene, poly(ethyl methacrylate), and poly(ethylene-co-

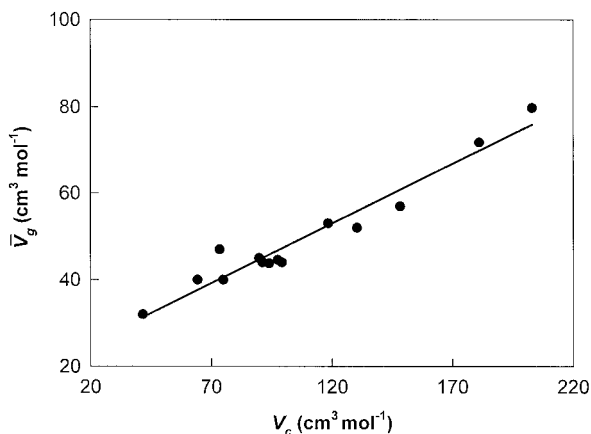


**Figure 3.** Correlation between the partial molar volume in rubbery polymers and the critical volume for various gases.

vinylacetate), and were taken from the literature.<sup>13,15–20</sup> The correlation in Figure 3 can be represented by

$$\bar{V}_g/\text{cm}^3 \text{ mol}^{-1} = 0.276 \times V_c + 19.8 \quad (9)$$

For glassy polymers, the solubilities are often expressed by the dual-mode equation<sup>21</sup>

$$C = k_d p + \left( \frac{C'_H b p}{1 + b p} \right) \quad (10)$$

where  $k_d$  is the Henry's law constant,  $b$  represents the interactions between the gas and the polymer, and  $C'_H$  is the hole saturation constant. For rubbery polymers,  $C'_H = 0$  and, so, eq. (10) reduces to the usual form of Henry's law.

Values of  $C$  were obtained by an iterative solution to eqs. (6), (8), and (10). To begin with,  $w_b$  was set to zero and values of  $C$  were fitted to eq. (10) to obtain the initial guesses for  $k_d$ ,  $C'_H$ , and  $b$ . This gave the initial value of  $\Delta V_d (=k_d p \bar{V}_g)$  for use in eq. (6), and thus a new set of  $C$  values from eq. (8) which were then fitted to eq. (10) to obtain the new set of dual-mode parameters. These iterations were continued until a unique set of dual-mode parameters was obtained. For temperatures above  $T_g$ , the calculation procedure was the same except that the iterations were carried out until a unique value for  $k_d$  was obtained.

## RESULTS AND DISCUSSION

Measurements on PS-CO<sub>2</sub> were made as a test case since precise results for this system have

been reported at 35°C using the pressure decay method.<sup>22</sup> Our results are compared with the literature values in Figure 4. There is a slight discrepancy between the two sets of data. This can be attributed to the different pressures used to condition the samples; our sample was conditioned with CO<sub>2</sub> at 50 atm whereas that reported in the literature was conditioned at 25 atm before starting solubility measurements. Consequently, our sample was a bit more dilated than the literature sample and, thus, exhibits slightly higher solubilities. Our values have also been corrected for matrix dilation whereas no such correction was applied in the other work. With these considerations, the agreement between the two sets of data is deemed to be quite good.

The sorption and desorption solubilities often show hysteresis in the glassy state due to the irreversible dilation of the polymer matrix during the first sorption run.<sup>13</sup> As seen in Figures 5 and 6, the dual-mode type<sup>21</sup> glassy nature of both PVC samples is not as evident during the sorption runs as it is during the desorption runs. The solubility curves for the two PVC samples are very similar; however, in the glassy region, the values for the UPVC sample are consistently higher than for the filled PVC sample even when the latter results are normalized with respect to 100% PVC. In the rubbery region, the solubilities in the two samples are about the same. Also, as seen in Figures 5 and 6, the onset of  $T_g$ , taken as the inflection point in the desorption isotherms, occurs at about 22 atm for FPVC and about 40 atm for UPVC. Thus, the additive in FPVC not only lowers the  $T_g$  but also reduces the amount of free volume that gets frozen-in at  $T_g$ . Some work is reported in the litera-

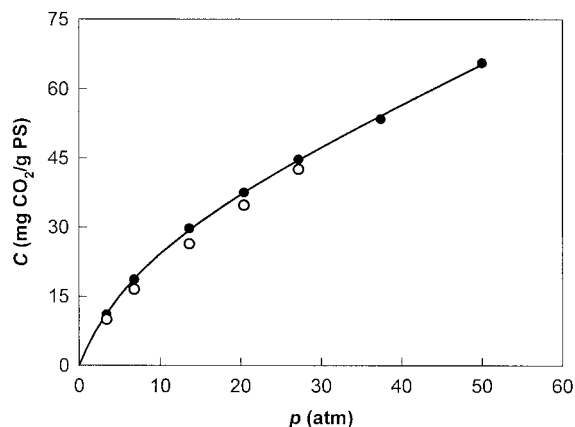


**Figure 4.** Solubility of CO<sub>2</sub> in PS at 35°C. ●—this work; ○—Morel and Paul.<sup>22</sup> The solid curve is drawn through the data points to aid the eye.

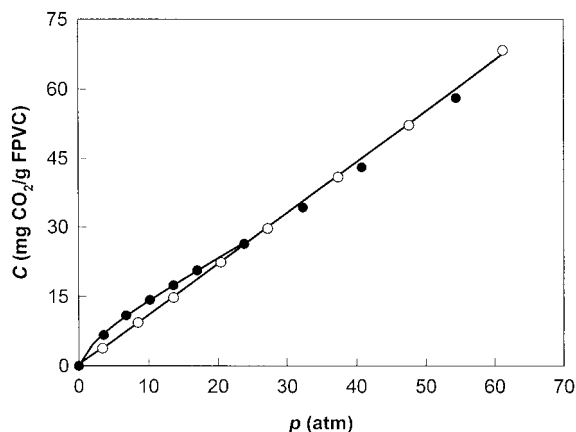


**Figure 5.** Solubility of  $\text{CO}_2$  in FPVC at  $35^\circ\text{C}$ .  $\circ$ —sorption run;  $\bullet$ —desorption run. Curves are drawn through the data points to show the trend.

ture on the solubility and diffusivity characteristics of  $\text{CO}_2$  in PVC. Equilibrium solubility values of  $75 \text{ mg CO}_2/\text{g polymer}$  at  $20^\circ\text{C}$ <sup>4</sup> and  $71 \text{ mg CO}_2/\text{g polymer}$  at  $25^\circ\text{C}$ <sup>5</sup> at 48 atm have been reported. These results were obtained by saturating the polymer in a pressure vessel and then weighing under ambient conditions. Our values of 52 and  $55 \text{ mg CO}_2/\text{g polymer}$  at  $35^\circ\text{C}$  and 48 atm determined in situ for FPVC and UPVC, respectively, are quite different from the literature values.

A typical desorption kinetic curve for FPVC- $\text{CO}_2$  as the pressure was decreased from 10.2 to 6.8 atm is shown in Figure 7. The discrete points are the measured values, and, to avoid clutter, only the data at selected intervals is shown. The solid curve through the data points is the fit in terms of eq. (3). The other solid curve in Figure

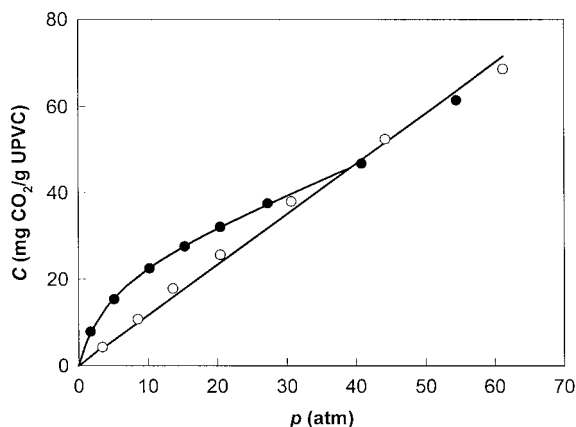


**Figure 6.** Solubility of  $\text{CO}_2$  in UPVC at  $35^\circ\text{C}$ .  $\circ$ —sorption run;  $\bullet$ —desorption run. Curves are drawn through the data points to show the trend.

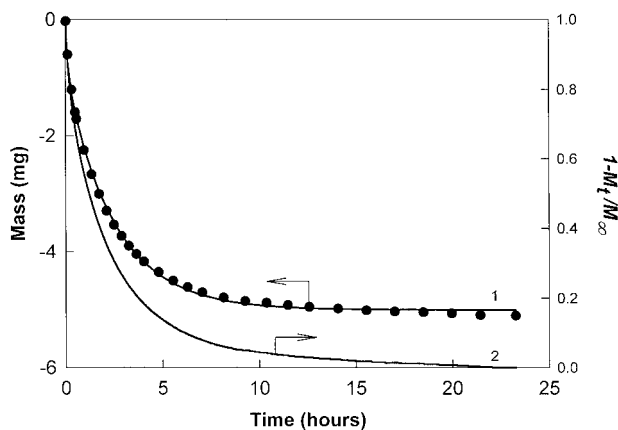


**Figure 7.** Desorption kinetics for the system FPVC- $\text{CO}_2$  at  $35^\circ\text{C}$  when the pressure was decreased from 10.2 to 6.8 atm.  $\bullet$ —measured values; curve 1 is the fit of the data points in terms of eq. (3); curve 2 is a plot of the data in terms of the function on the right hand side of eq. (4).

7 is the plot for the right-hand side of eq. (4), and the moment  $\tau$  is simply given by the area under this curve. The diffusion coefficients calculated by the two techniques from analysis of the desorption data for the FPVC- $\text{CO}_2$  system at various pressures are shown in Figure 8, where the values of  $D$  are plotted against the average concentration corresponding to the pressures before and after the desorption step. For the most part, there is excellent agreement between the two techniques. The hybrid method does consistently yield slightly higher values than the moment method and does

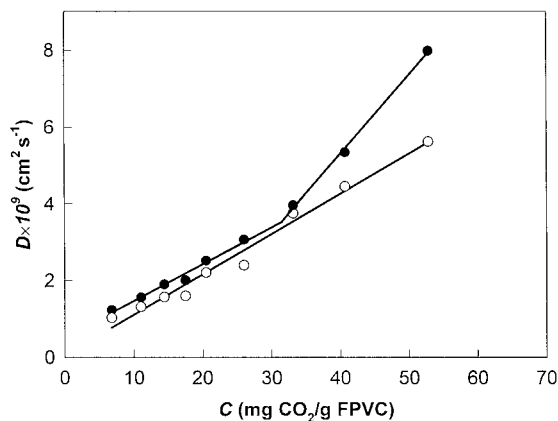


**Figure 8.** A comparison of the diffusion coefficients obtained using the hybrid method, eq. (3), and the moment method, eq. (5), for  $\text{CO}_2$  in FPVC at  $35^\circ\text{C}$  as a function of average concentration. The values shown are from the desorption runs.  $\bullet$ —hybrid method;  $\circ$ —moment method.

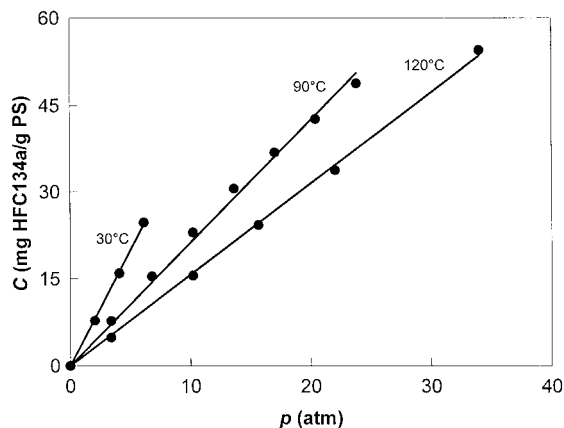


**Figure 9.** Solubility of HFC134a in PS at 30, 90, and 120°C. For each temperature, a curve is drawn through the data points to show the trend.

capture the fine details of gas transport in terms of identifying the onset of plasticization at about 30 atm. Errors in using the moment method can arise if an accurate value of  $M_\infty$  is not known and if the kinetic run is stopped short of reaching equilibrium. On the other hand, the hybrid method can be used to determine  $M_\infty$  while simultaneously determining the diffusion coefficient.

Literature values of infinite dilution diffusion coefficient of CO<sub>2</sub> in PVC are  $8 \times 10^{-9} \text{ cm}^2 \text{ s}^{-1}$  at 35°C determined from permeability time lags,<sup>23</sup> and  $2 \times 10^{-9} \text{ cm}^2 \text{ s}^{-1}$  at 25°C<sup>5</sup> and  $1.3 \times 10^{-8} \text{ cm}^2 \text{ s}^{-1}$  at 20°C and 48 atm<sup>4</sup> determined from sorption kinetics using eq. (1) truncated after the first term on the right-hand side. We obtained values of  $0.8 \times 10^{-9}$  and  $0.3 \times 10^{-9} \text{ cm}^2 \text{ s}^{-1}$  for the infinite dilution diffusion coefficient of CO<sub>2</sub> in FPVC and UPVC, respectively; in general, the diffusion coefficients were found to be higher for FPVC than for UPVC due to the plasticizing effect of the additive in FPVC. Our values are about an order of magnitude lower than those reported by Berens and Huvard.<sup>5</sup> It should be noted that, in the latter case, the low pressure results were obtained using an electrobalance, the high pressure results were obtained by weighing the samples under ambient conditions, and there was considerable scatter in the derived diffusion coefficients. The large scatter in diffusion coefficients found among the literature values may also be due to the varying amounts and the different kinds of additive in the PVC samples used.

The equilibrium solubilities of HFC134a in PS were determined at three temperatures and the results plotted against pressure are shown in Figure 9. The lines drawn in Figure 9 are meant

only to show trends in the results. At 30 and 90°C where HFC134a is subcritical, the shape of the isotherms was found to be the same when solubilities were plotted against fugacity or activity of HFC134a. The plasticization effect of HFC134a on PS is quite small. The  $T_g$  is depressed to 88°C at 20 atm.<sup>24</sup> Thus, the sorption isotherms at 30 and 90°C would be expected to show dual-mode type behavior similar to that seen for PS-CO<sub>2</sub> in Figure 4. However, as seen in Figure 9, no such distinct dual-mode behavior is observed. The absence of the dual-mode character at 30°C may be due to the rather limited pressure range available. At 90°C, a slight curvature is seen and this diminished dual-mode signature may be due to the proximity of the system to its  $T_g$ . It is also possible that the relatively large size of HFC134a prevents it from entering the Langmuirian sites. This is reflected in the low diffusion rates of HFC134a in glassy PS obtained from the sorption kinetics. At 30 and 90°C, the diffusion coefficients showed almost no dependence on concentration. The average values of  $D$  obtained at 30 and 90°C are  $4.1 \times 10^{-11}$  and  $6.7 \times 10^{-10} \text{ cm}^2 \text{ s}^{-1}$ , respectively. At 120°C, the diffusion coefficients are 2–3 orders of magnitude higher and showed a weak pressure dependence; the  $D$  values increased from  $1.2 \times 10^{-8} \text{ cm}^2 \text{ s}^{-1}$  at infinite dilution to about  $3.6 \times 10^{-8} \text{ cm}^2 \text{ s}^{-1}$  at 35 atm.

The *in situ* technique described here can be used for a variety of gases and vapors, is fast, and provides highly precise values of solubility and diffusivity. Measurements over extended ranges of temperature and pressure on the solubility and diffusivity of blowing agents for producing polymeric foams are now being carried out, and will be reported in forthcoming articles.

The authors thank Floyd Toll and Graham McLaurin for the technical assistance provided during the equipment set-up. This study was issued as NRCC No. 41965.

## REFERENCES AND NOTES

1. R. M. Felder, *J. Membr. Sci.*, **3**, 15 (1978).
2. C. M. Balik, *Macromolecules*, **29**, 3025 (1996).
3. W. J. Koros, A. H. Chan, and D. R. Paul, *J. Membr. Sci.*, **2**, 165 (1977).
4. V. Kumar, J. E. Weller, and R. Montecillo, *SPE ANTEC Tech. Papers*, **38**, 1452 (1992).
5. A. R. Berens and G. S. Huvard, *ACS Symp. Ser.*, **406**, 207 (1989).



6. W. J. Koros, D. R. Paul, and A. Rocha, *J. Polym. Sci. Polym. Phys. Ed.*, **14**, 687 (1976).
7. Y. Kamiya, T. Hirose, K. Mizoguchi, and Y. Naito, *J. Polym. Sci.: Part B: Polym. Phys.*, **24**, 1525 (1986).
8. Y. P. Handa, J. Roovers, and P. Moulinié, *J. Polym. Sci.: Part B: Polym. Phys.*, **35**, 2355 (1997).
9. S. Angus, B. Armstrong, and K. M. De Reuck, eds., *Int. Thermodyn. Tables of the Fluid State, Carbon Dioxide*, Vol. 3, Pergamon Press, New York, 1976.
10. J. M. Prausnitz, R. N. Lichtenthaler, and E. G. De Azevedo, *Molecular Thermodynamics of Fluid-Phase Equilibria*, Prentice-Hall, Englewood, NJ, 1986.
11. J. H. Dymond and E. B. Smith, *The Virial Coefficients of Pure Gases and Mixtures*, Clarendon Press, Oxford, 1980.
12. S. S. Jordan and W. J. Koros, *Macromolecules*, **28**, 2228 (1995).
13. Y. Kamiya, K. Terada, K. Mizoguchi, and Y. Naito, *Macromolecules*, **25**, 4321 (1992).
14. R. C. Reid, J. M. Prausnitz, and B. E. Poling, *The Properties of Gases and Liquids*, McGraw-Hill, New York, 1987.
15. G. K. Fleming and W. J. Koros, *Macromolecules*, **19**, 2285 (1986).
16. Y. Kamiya, T. Hirose, Y. Naito, and K. Mizoguchi, *J. Polym. Sci.: Part B: Polym. Phys.*, **26**, 159 (1988).
17. G. K. Fleming and W. J. Koros, *J. Polym. Sci.: Part B: Polym. Phys.*, **28**, 1137 (1990).
18. Y. Kamiya, Y. Naito, T. Hirose, and K. Mizoguchi, *J. Polym. Sci.: Part B: Polym. Phys.*, **28**, 1297 (1990).
19. Y. Kamiya, K. Mizoguchi, and Y. Naito, *J. Membr. Sci.*, **93**, 45 (1994).
20. Y. Kamiya, Y. Naito, and D. Bourbon, *J. Polym. Sci.: Part B: Polym. Phys.*, **32**, 281 (1994).
21. W. R. Vieth, J. M. Howell, and J. H. Hsieh, *J. Membr. Sci.*, **1**, 177 (1976).
22. G. Morel and D. R. Paul, *J. Membr. Sci.*, **10**, 273 (1982).
23. B. P. Tikhomirov, H. B. Hopfenberg, V. Stannett, and J. L. Williams, *Makromol. Chem.*, **118**, 117 (1968).
24. Z. Zhang and Y. P. Handa, *J. Polym. Sci.: Part B: Polym. Phys.*, **36**, 977 (1998).